Neutron-proton weak coupling: Reducing shell-model dimensions by truncations in the neutron and proton subspaces

A. Etchegoyen,* M. C. Etchegoyen,* and B. H. Wildenthal†
Department of Physics and Atmospheric Science, Drexel University, Philadelphia, Pennsylvania 19104
(Received 4 May 1988)

A scheme for shell-model truncations based on diagonalizing and then truncating the separate neutron and proton subspaces and then combining the truncated subspaces together for rediagonalization is described and evaluated. Projected *m*-scheme techniques are used for these calculations and aspects of this technique relevant to this application are discussed. Detailed calculations are made for ^{20}Ne and ^{21}Ne. The truncated results for level schemes, $B(E2)$ values, and wave-function amplitude distributions are compared with the results of calculations in the analogous full shell-model basis spaces. The results suggest that the neutron-proton "weak-coupling" approach may be an effective truncation scheme even though it is known that the *n-p* interaction has a dominating influence on these nuclei.

I. INTRODUCTION

The nuclear shell model has evolved to the stage that it can be used to make systematic studies of fundamental features such as electromagnetic moments and transition probabilities, beta decay rates, and such complex phenomena as isospin mixing and parity violation.[1] Such successes are limited, however, to regions of nuclei for which shell-model dimensionalities are small enough to be manageable in explicit calculations. In order to make shell-model calculations more generally applicable, techniques for reducing the model state dimensions must be developed.

In the present work we study a truncation approach based on diagonalizing the separate neutron and proton subspaces of a total shell-model space. The lowest-lying neutron and proton eigenvectors which result are then combined to form a new space for the total number of active particles and this new space is rediagonalized to "weakly" couple the neutron and proton results into the full solution. Of course, the coupling is in one sense certainly not weak, but the hope is that the low-lying eigenvectors of the untruncated space will turn out to have large overlaps with the eigenvectors of the space constructed from the low-lying eigenvectors of the separate neutron and proton spaces. The aims of this work are to develop a technique for making such calculations and evaluate the results by comparing them to corresponding results obtained in the analogous untruncated model spaces.

Previous work along these lines has been reported by Arima and Hamamoto,[2] Wong and Zucker,[3] McGrory,[4] and Chiang, Wang, and Hsieh.[5] The work of Arima and Hamamoto[2] concerned the particle-hole states near ^{16}O. In this case the two subspaces contain particles from different shells, a situation which is the traditional realm of weak-coupling calculations. The same approach can in principle also be applied in cases for which the particles in the two subspaces occupy the same orbits. For example, the states of ^{20}Ne could be modeled in terms of the products of the states of ^{18}F:

$$|\,^{20}\mathrm{Ne}\rangle = |\,^{18}\mathrm{F},J_iT_i\rangle \times |\,^{18}\mathrm{F},J_jT_j\rangle\ . \tag{1}$$

This direct-product approach in general does not produce states with good J and T values and the basis generated is overcomplete.

McGrory[4] proposed a truncation scheme for heavy nuclei in which neutrons and protons would occupy two unconnected subspaces. In this context, states of ^{20}Ne would be modeled in terms of the products of ^{18}O and ^{18}Ne states,

$$|\,^{20}\mathrm{Ne},J\rangle = [\,|\,^{18}\mathrm{Ne},J_iT_i\rangle \times |\,^{18}\mathrm{O},J_jT_j\rangle\,]^J\ , \tag{2}$$

but there would still be problems with nonconservation of isospin in the final space. Chiang, Wang, and Hsieh[5] have applied the McGrory approach to describe the $N=81$ and 83 isotopes. In this case the product wave functions will have good J and T values since the protons and neutrons occupy completely different orbits.

The neutron-proton weak-coupling truncation method we describe here is based on the projection operator approach used in the shell-model code OXBASH.[6] It produces wave functions with good J and T values. The method starts with separating the original shell-model space for N active particles into neutron (N_n particles) and proton (N_p particles) subspaces. The *nn* and *pp* components of the model Hamiltonian are then diagonalized in the respective subspaces to produce spectra of low-lying neutron and proton eigenstates $N_nJ_iT_i$ and $N_pJ_jT_j$.

Next, N-particle basis states are generated as the products of the low-lying neutron and proton eigenstates

$$|\,N\rangle = |\,N_nJ_{n_i}T_{n_i}\rangle \times |\,N_pJ_{p_j}T_{p_j}\rangle\ . \tag{3}$$

These product basis states again in general will not have good J and T values. However, a basis with good J and T can be obtained from them by applying the projection operator P^{JT} which is a product operator composed

of independent J and T projection operators. ($P^{JT}=P^{J}P^{T}$.) The J-projection operator is defined by

$$P^{J}=\prod_{\substack{J'=J_{\min}\\ J'\neq J}}^{J_{\max}} \frac{\hat{J}_{0p}^{2}-J'(J'+1)}{J(J+1)-J'(J'+1)} \tag{4}$$

where $J_{\min}$ and $J_{\max}$ are the two limits of the triangular coupling $\vec{J}=\vec{J}_{n_i}+\vec{J}_{p_j}$ [see Eq. (3)]. The isospin operator is defined similarly.

The basis states produced by projection, though having good J and good T, are not orthonormal. Orthogonality and normalization is obtained by an explicit Gram-Schmidt procedure. The Gram-Schmidt procedure also provides a check on linear dependence of the basis states.

The procedures just described are the natural mode of operation for an m-scheme computer code such as OXBASH which is designed to diagonalize in a good J and T basis which has been projected from an m-scheme basis defined in terms of J_z and T_z. The next step in our method, as in the general OXBASH application, is to use the orthogonal set of basis vectors with good J and T values to construct the corresponding Hamiltonian matrices, which can then be diagonalized, typically with the Lanczos technique.[7] We haved implemented this truncation concept by writing a set of supplemental codes for OXBASH which accomplish the tasks of working with the initial subspaces, truncating them, and then forming the product-state model basis. In the following sections we will examine some results obtained with these codes.

II. DISCUSSION

Application of this method to the *sd* shell commences by expressing the model Hamiltonian[8] in neutron-proton notation,

$$H=H_{pp}+H_{nn}+H_{np} \ . \tag{5}$$

Wave functions in the two subspaces are obtained by solving the equations

$$H_{pp}\,|\,\Psi_i^{p}\rangle=\epsilon_i^{p}\,|\,\Psi_i^{p}\rangle \tag{6}$$

and

$$H_{nn}\,|\,\Psi_j^{n}\rangle=\epsilon_i^{n}\,|\,\Psi_j^{n}\rangle \tag{7}$$

where for ^{20}Ne the neutron wave functions would correspond to the eigenstates of ^{18}O and the (mirror) proton states to those of ^{18}Ne. For ^{21}Ne the neutron states would instead correspond to the eigenstates of ^{19}O.

The product-state basis is formed by

$$|\,\Psi_{ij}^{pn}\rangle=|\,I_k\rangle=|\,\Psi_i^{p}\rangle\times|\,\Psi_j^{n}\rangle \ . \tag{8}$$

The projection operator is then applied to these product vectors $|\,I_k\rangle$ to generate (after orthogonalization) the new orthonormal basis states $|\,O_i\rangle$

$$|\,O_i\rangle=\sum_{k=1}^{i}\alpha_{ik}P^{JT}\,|\,I_k\rangle \ . \tag{9}$$

At this stage, there are two bases: the good-JT basis, the $|\,O_i\rangle$ vectors, and the OXBASH m-scheme basis over which the $|\,O_i\rangle$ vectors are expanded. The m-scheme basis spans the complete space for N particles. Our truncations are performed in the good-JT space of Eq. (9).

The Hamiltonian matrix is generated from the $|\,O_i\rangle$ as

$$\begin{aligned}H_{ij}=\langle O_i\,|\,H\,|\,O_j\rangle&=\sum_k\alpha_{jk}\langle O_j\,|\,P^{JT}H\,|\,I_k\rangle\\&=\sum_k\alpha_{jk}\langle O_i\,|\,H\,|\,I_k\rangle\\&=\sum\alpha_{jk}[\langle O_i\,|\,I_k\rangle\xi_k\\&\qquad+\langle O_i\,|\,H_{np}\,|\,I_k\rangle]\\&=\xi_i\delta_{ij}+\sum_k\alpha_{jk}\langle O_i\,|\,H_{np}\,|\,I_k\rangle \ ,\end{aligned} \tag{10}$$

where ξ_i is the sum of the binding energies of the valence particles shown in Eqs. (6) and (7). The same result would be obtained by applying H to $|\,O_k\rangle$ rather than to $|\,I_k\rangle$, but applying the Hamiltonian to $|\,I_k\rangle$ speeds up the calculation.

A. Applications to ^{20}Ne

^{20}Ne is a good nucleus with which to test this method, since the n-p interaction is known to be strong and to be responsible for the rotational features of its spectrum. This allows the truncation scheme to be inspected in an unfavorable situation. The dimension of ^{18}O (^{18}Ne) in the

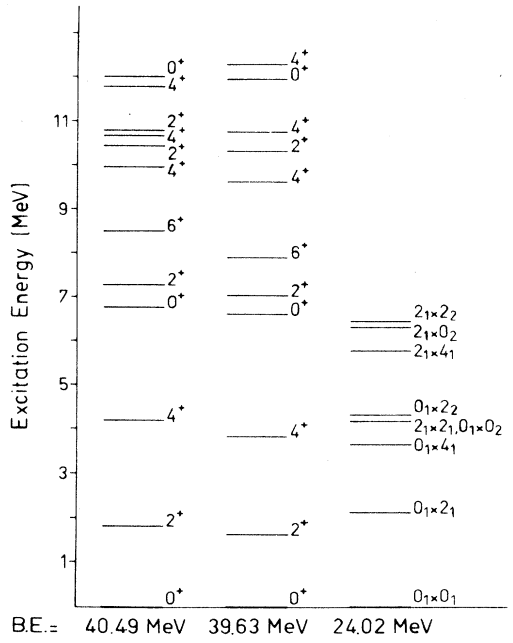

FIG. 1. Excitation energies of states of ^{20}Ne. The first column shows the results obtained in the full *sd*-shell space, the center column shows the results obtained after truncating in the neutron and proton spaces and then rediagonalizing in the product space, and the third column shows the energies associated with the product basis vectors. The binding energies of the ground states are shown below each column.

TABLE I. Comparisons of state dimensions in the full and truncated shell-model spaces.

	Mass 20				Mass 21			
J^π	0^+	2^+	4^+	6^+	$\frac{1}{2}^+$	$\frac{3}{2}^+$	$\frac{5}{2}^+$	$\frac{7}{2}^+$
Full shell-model dimension	21	56	44	17	109	188	223	209
Truncated dimension	9	14	14	7	24	42	51	47
Reduction factor	2.3	4	3.1	2.4	4.5	4.5	4.4	4.4

m scheme is 14 for the sd space, split into three 0^+, two 1^+, five 2^+, two 3^+, and two 4^+ states. For any particular total JT combination the product basis will therefore consist of 196 (14×14) states. When T projection is applied it can be seen that the number of independent states is reduced to $105=n(n+1)/2$. From each product state one can project, in principle, as many good-JT states as allowed by the triangle rules. If a $J=2$ state is taken for both the ^{18}O and ^{18}Ne states, states with angular momentum 0,1,2,3,4 and with isospins 0,1,2 could be obtained in mass 20, that is, a maximum number of 15 states from only a single product wave function.

We choose as a truncation for ^{20}Ne to restrict the $A=18$ states used in forming the product basis states to the lowest two states each of spins $J=0$, 2, and 4. The product basis therefore has dimension $21=(6\times 7)/2$. The effects of thus truncating the basis will be studied by comparisons of energy levels, $B(E2)$ values and overlaps with both exact shell-model wave functions and with the product wave-function vectors $|I_k\rangle$. Energy-level comparisons are displayed in Fig. 1. The first column of Fig. 1 shows the results of the exact shell-model diagonalization. The third column of Fig. 1 shows the energies corresponding to the original simple product wave functions; these wave functions have neither good J nor good T. The spectrum is quite different from the exact calculation, clearly showing the importance of the H_{np} interaction. This is further reaffirmed by comparing the ground-state valence-particle binding energies: 24.34 MeV for the simple product wave function and 40.49 MeV for the exact calculation, that is 16.65 MeV of extra binding is produced by the np interaction. The center column of Fig. 1 shows the result diagonalizing in the projected and orthonormalized product space after truncating each of the neutron and proton subspaces to only two states each of $J=0^+$, 2^+, and 4^+. The ground-state rotation band ($0^+,2^+,4^+,6^+$) is reproduced and so are other states up to ≈ 10 MeV of excitation energy. In Table I the full shell-model and weak-coupling truncation model dimensions are shown for different J values.

A better test of the effectiveness of this truncation might be a comparison of $E2$ transition probabilities, since these features emphasize the configuration mixing and collectivity in the ^{20}Ne wave functions. Table II shows such a comparison for $B(E2)$ transitions. The correspondence is quite satisfactory and it seems that the collective natures of the full-space states emerge largely undiminished through the truncations. The $B(E2)$ results are reflected in a direct examination of the wave functions themselves. Overlaps between the truncated and untruncated wave functions are shown in Table III. For a nontruncated weak-coupling basis this overlap ma-

TABLE II. Comparison of $B(E2)$ values as calculated with the full and truncated wave functions for ^{20}Ne and ^{21}Ne. (Integer spins correspond to transitions in ^{20}Ne and half-integer spins to transitions in ^{21}Ne.)

	$B(E2)$ (e^2fm^4)				
	Full space	Truncated		Full space	Truncated
$2_1^+\rightarrow 0_1^+$	60.6	57.8	$\frac{7}{2}_2^+\rightarrow\frac{5}{2}_1^+$	0.5	0.8
$2_2^+\rightarrow 0_2^+$	17.0	16.5	$\frac{7}{2}_1^+\rightarrow\frac{5}{2}_2^+$	7.1	7.0
$4_1^+\rightarrow 2_1^+$	72.2	71.3	$\frac{7}{2}_2^+\rightarrow\frac{5}{2}_2^+$	32.5	21.5
$4_2^+\rightarrow 2_2^+$	7.2	7.8	$\frac{7}{2}_1^+\rightarrow\frac{5}{2}_3^+$	1.9	2.0
$6_1^+\rightarrow 4_1^+$	55.9	57.2	$\frac{7}{2}_2^+\rightarrow\frac{5}{2}_3^+$	31.0	41.4
			$\frac{7}{2}_1^+\rightarrow\frac{3}{2}_1^+$	46.0	44.2
$\frac{5}{2}_1^+\rightarrow\frac{3}{2}_1^+$	110.5	110.6	$\frac{7}{2}_2^+\rightarrow\frac{3}{2}_2^+$	5.1	3.5
$\frac{5}{2}_2^+\rightarrow\frac{3}{2}_1^+$	1.8	0.2	$\frac{5}{2}_2^+\rightarrow\frac{1}{2}_1^+$	31.9	36.0
$\frac{5}{2}_3^+\rightarrow\frac{3}{2}_1^+$	2.8	0.9	$\frac{5}{2}_3^+\rightarrow\frac{1}{2}_1^+$	20.2	15.0
$\frac{7}{2}_1^+\rightarrow\frac{5}{2}_1^+$	74.1	71.0	$\frac{3}{2}_2^+\rightarrow\frac{3}{2}_1^+$	4.1	4.7

TABLE III. Overlap values of the wave functions of 0^+, 2^+, 4^+, and 6^+ states in ^{20}Ne as calculated in the truncated space (lowest nine states of each J) and the full space (lowest two states of each J). The elements of the overlap matrices are labeled by the excitation energies of the states.

Full MeV	Truncated MeV	0.0	6.6	11.9	15.1	16.0	16.5	20.3	23.9	28.1
	$J=0$									
0.0		95.0%	0.0%	0.0%	0.0%	0.0%	0.0%	0.0%	0.1%	0.0%
6.8		0.1%	95.8%	0.1%	0.0%	0.0%	0.0%	0.0%	0.0%	0.0%
Full MeV	Truncated MeV	1.6	7.0	10.3	12.7	13.9	14.4	16.3	17.9	18.1
	$J=2$									
1.8		96.2%	0.0%	0.0%	0.0%	0.0%	0.0%	0.0%	0.0%	0.1%
7.3		0.0%	96.4%	0.0%	0.1%	0.0%	0.0%	0.0%	0.0%	0.0%
Full (MeV)	Truncated (MeV)	3.8	9.6	10.7	12.3	13.6	16.0	17.0	19.3	19.7
	$J=4$									
4.2		96.8%	0.0%	0.0%	0.0%	0.0%	0.0%	0.0%	0.0%	0.0%
10.0		0.1%	93.8%	0.0%	0.4%	0.0%	0.2%	0.1%	0.0%	0.1%
Full (MeV)	Truncated (Mev)	7.9	13.0	14.4	16.6	18.3	20.1	27.2		
	$J=6$									
8.5		97.8%	0.0%	0.0%	0.0%	0.0%	0.0%	0.0%		

trix would be the identity matrix. It is observed that the wave functions resulting from the truncation closely reproduce the full-space results up to approximately 10 MeV, with all overlaps greater than 0.97.

In Table III it can be seen that the lower full shell-model states are seen to have little overlap with any of the higher-lying weak-coupling model states, and this gives rise to the question of whether the present weak-coupling basis could be truncated further. This is assessed by looking at the overlaps, shown in Table IV, of the weak-coupling wave functions with the nonorthogonal $|I_k,J,T\rangle = P^{JT}|I_k\rangle$ good-JT product basis states. It appears from Table IV that the basis could be truncated by at least a further 20%. Note that, since $|I_k,J,T\rangle$ is a nonorthogonal basis, the percentages shown in Table IV are strictly valid only within a row, that is, when $|I_k,J,T\rangle$ is expanded in terms of JT weak-coupling wave functions, whereas they would be upper limits when

TABLE IV. Overlaps of the wave functions of ^{20}Ne obtained from diagonalizations in the truncated space with the basis vectors of the product space. The product states were projected into good-JT form before the overlaps with the eigenstates were evaluated.

Truncation eigenstates		0_1	0_2	2_1	2_2	4_1	4_2	6_1
Product states	(J,T)	(0,0)		(2,0)		(4,0)		(6,0)
$0_1\times0_1$		58.2%	7.1%					
$0_1\times2_1$				64.5%	12.9%			
$0_1\times4_1$						35.7%	0.5%	
$0_1\times0_2$		1.1%	70.2%					
$2_1\times2_1$		42.4%	0.4%	18.4%	17.1%	35.9%	45.9%	
$0_1\times2_2$				4.8%	61.4%			
$2_1\times4_1$				21.9%	0.0%	23.2%	10.6%	79.4%
$2_1\times0_2$				1.5%	8.3%			
$2_1\times2_2$		6.6%	37.1%	5.3%	7.8%	5.8%	6.2%	
$4_1\times4_1$		8.9%	6.5%	2.3%	3.2%	3.3%	0.5%	5.1%
$4_1\times0_2$						0.0%	3.4%	
$4_1\times2_2$				2.5%	3.6%	0.1%	42.9%	2.9%
$0_2\times0_2$		0.9%	3.1%					
$0_2\times2_2$				0.9%	0.1%			
$2_2\times2_2$		2.6%	0.4%	0.1%	0.6%	1.2%	0.0%	
$0_1\times4_2$						11.9%	10.2%	
$2_1\times4_2$				6.4%	0.8%	8.4%	4.2%	12.0%
$4_1\times4_2$		7.4%	3.7%	2.2%	5.4%	1.8%	0.5%	3.6%
$0_2\times4_2$						0.0%	1.7%	
$2_2\times4_2$				1.0%	1.5%	0.1%	7.8%	1.4%
$4_2\times4_2$		1.4%	1.1%	0.4%	1.7%	0.3%	0.6%	0.9%

any given weak-coupling wave function is expanded in terms of the $|I_k,J,T\rangle$ basis set. As an example, the weak-coupling ^{20}Ne ground-state total percentage adds up to 129.5%, a clear indication of the nonorthogonality of the product basis.

Note that the $|0_1^+\times 0_1^+,J^\pi=0^+,T=0\rangle$ basis state (i.e., the product of ^{18}Ne and ^{18}O ground states) has a 58% overlap with the weak-coupling ^{20}Ne ground state, 7% with a second 0^+ state, and therefore 35% with the remaining 0^+ states of ^{20}Ne, which lie above 10 MeV of excitation energy. This is a considerable splitting of the strength and it reaffirms the importance of the neutron-proton interaction. These overlaps are of further interest in order to gain insight into the structure of ^{20}Ne as a function of ^{18}O and ^{18}Ne. None of the weak-coupling states has a single main component from the nonorthogonal basis, but the mixing from this basis set typically does not extend beyond two or three major components.

B. Application to ^{21}Ne

The truncation for ^{21}Ne was chosen differently from that used for ^{20}Ne. Instead of a fixed number of subspace states, an upper limit of 10 MeV excitation energy was set on the product-state energies. All possible spins were thereby included in the product basis, i.e., $\frac{1}{2}^+$, $\frac{3}{2}^+$, $\frac{5}{2}^+$, $\frac{7}{2}^+$, $\frac{9}{2}^+$, and $\frac{11}{2}^+$ for mass 19 and 0^+, 1^+, 2^+, 3^+, and 4^+ for mass 18.

A comparison of energy spectra for ^{21}Ne is shown in Fig. 2 and the dimension-reduction factors from the truncation are listed in Table I. The difference in binding energy of the valence particles between the full and truncated calculations is 800 keV. The $B(E2)$ transition rates from the two calculations are shown in Table II. Transitions between the second and the third $\frac{5}{2}^+$ states and the second $\frac{7}{2}^+$ states show the most difference between full and truncated results. These differences are about 30%, although the sums of the two transition rates are approximately 63 e^2 fm^4 for both models.

The weak-coupling truncation approximation in ^{21}Ne is seen to yield energies close to the full-space results up

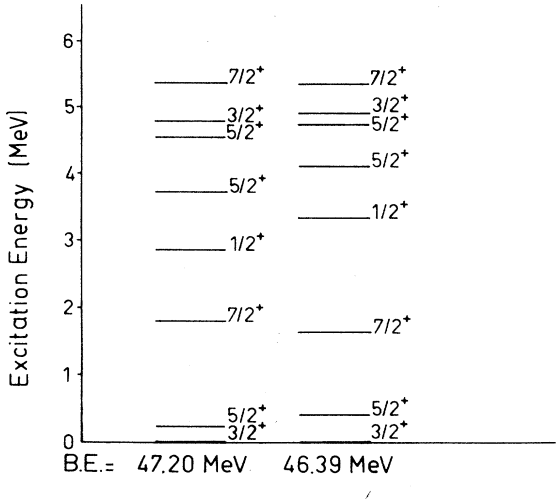

FIG. 2. Excitation energies of states of ^{21}Ne. The first column shows the full-*sd*-shell results and the second column shows the neutron-proton truncation results.

TABLE V. Overlap values of the wave functions of the $\frac{3}{2}^+$, $\frac{1}{2}^+$, $\frac{5}{2}^+$, and $\frac{7}{2}^+$ states of ^{21}Ne as calculated in the truncated space and the full space. The presentation is the same as that of Table III.

Full (MeV)	Truncation (MeV)	0.0	4.9	6.2	7.3	8.1	9.4	10.2	10.8	11.8
	$J=\frac{3}{2}$									
0.0		95.1%	0.0%	0.0%	0.0%	0.0%	0.0%	0.0%	0.0%	0.0%
4.8		0.0%	88.1%	0.6%	0.8%	1.1%	0.6%	0.0%	0.0%	0.0%
Full (MeV)	Truncation (MeV)	3.3	7.0	7.9	9.8	10.7	10.9	11.6	14.2	15.0
	$J=\frac{1}{2}$									
2.9		89.7%	0.1%	1.2%	0.1%	0.0%	0.1%	0.0%	0.0%	0.0%
Full (MeV)	Truncation (MeV)	0.4	4.1	4.7	7.4	8.1	9.0	9.3	10.2	10.5
	$J=\frac{5}{2}$									
0.2		92.9%	0.1%	0.3%	0.0%	0.0%	0.0%	0.0%	0.1%	0.0%
3.7		0.3%	90.3%	0.9%	0.1%	0.1%	0.0%	0.0%	0.0%	0.0%
4.6		0.5%	1.1%	90.9%	0.3%	0.0%	0.1%	0.1%	0.2%	0.0%
Full (MeV)	Truncation (MeV)	1.6	5.3	6.2	7.4	8.0	9.4	9.7	10.2	10.4
	$J=\frac{7}{2}$									
1.8		95.5%	0.2%	0.0%	0.0%	0.0%	0.0%	0.0%	0.0%	0.0%
5.4		0.4%	93.5%	0.3%	0.1%	0.0%	0.1%	0.0%	0.0%	0.1%

TABLE VI. Overlaps of the wave functions of ^{21}Ne obtained from diagonalizations in the truncated space with the basis vectors of the product space. The product states were projected into good-JT form before the overlaps with the eigenstates were evaluated.

Truncation eigenstates	$\frac{3}{2}_1$	$\frac{3}{2}_2$	$\frac{1}{2}_1$	$\frac{5}{2}_1$	$\frac{5}{2}_2$	$\frac{5}{2}_3$	$\frac{7}{2}_1$	$\frac{7}{2}_2$
Product states (J,T)	$(\frac{3}{2},\frac{1}{2})$		$(\frac{1}{2},\frac{1}{2})$		$(\frac{5}{2},\frac{1}{2})$		$(\frac{7}{2},\frac{1}{2})$	
$\frac{5}{2}_1\times 0_1$				50.4%	12.4%	0.6%		
$\frac{3}{2}_1\times 0_1$	60.0%	0.5%						
$\frac{1}{2}_1\times 0_1$			66.5%					
$\frac{5}{2}_1\times 2_1$	51.0%	6.8%	1.0%	0.1%	29.5%	19.7%	34.2%	11.2%
$\frac{3}{2}_1\times 2_1$	18.2%	0.9%	11.1%	37.1%	3.3%	7.3%	24.8%	11.9%
$\frac{7}{2}_1\times 0_1$							31.1%	14.8%
$\frac{5}{2}_2\times 0_1$				2.1%	36.3%	15.6%		
$\frac{1}{2}_1\times 2_1$	0.1%	30.3%		0.0%	19.5%	24.5%		
$\frac{5}{2}_1\times 4_1$	1.6%	0.6%		11.6%	3.7%	14.0%	4.8%	25.9%
$\frac{3}{2}_1\times 0_1$	1.4%	30.0%						
$\frac{3}{2}_1\times 4_1$				1.8%	0.0%	4.0%	12.8%	10.7%
$\frac{9}{2}_1\times 2_1$				8.6%	2.9%	1.2%	5.9%	23.8%
$\frac{7}{2}_1\times 2_1$	12.0%	7.0%		11.9%	2.1%	7.3%	4.7%	1.4%
$\frac{5}{2}_2\times 2_1$	3.0%	7.4%	34.1%	0.7%	1.4%	15.2%	1.4%	2.2%
$\frac{3}{2}_3\times 0_1$	0.1%	15.7%						
$\frac{3}{2}_2\times 2_1$	0.9%	7.4%	10.5%	1.2%	2.7%	1.0%	0.9%	0.1%
$\frac{7}{2}_2\times 0_1$							3.3%	10.0%

to approximately 5.5 MeV. This is not as large an energy interval as for ^{20}Ne (10 MeV), probably due to the level density being larger for odd-even nuclei. There are seven shell-model states in ^{20}Ne in 10 MeV of excitation while there are ten $T=\frac{1}{2}$ states in ^{21}Ne in 5.5 MeV of excitation. (There are 45 $T=\frac{1}{2}$ shell-model states with excitation energies below 10 MeV in ^{21}Ne.)

The overlaps between the truncated and the full-space shell-model wave functions for ^{21}Ne are shown in Table V and, in Table VI, the overlaps of weak-coupling wave functions with good-JT product basis states are displayed. As for ^{20}Ne, these overlaps serve a double purpose: First, they give information on the structure of ^{21}Ne in terms of ^{18}Ne and ^{19}O; second, they assess whether or not the product basis can be truncated any further without substantial loss in the weak-coupling wave functions. Again, only a few expansion coefficients are large, indicating that a further truncation might be feasible.

TABLE VII. Comparison of energies and state dimensions of states of ^{20}Ne and ^{21}Ne as obtained in the full space, the truncated space with good-JT, values and the truncated space without good-JT values. The values for the ground states are binding energies. The values for excited states are excitation energies.

J^π	Full space (MeV)	Dim	Good T (MeV)	Truncation Dim	Bad T (MeV)	Truncation Dim
0^+	40.49	21	39.63	9	39.31	12
	6.76		6.56		6.56	
2^+	1.78	56	1.57	14	1.45	24
	7.32		6.97		7.00	
4^+	4.21	44	3.82	14	3.59	24
	9.98		9.57		9.36	
6^+	8.52	17	7.88	7	7.57	12
$\frac{3}{2}^+$	47.20	188	46.39	42	45.79	42
	4.79		4.88		5.01	
$\frac{1}{2}^+$	2.87	109	3.26	24	3.55	24
$\frac{5}{2}^+$	0.25	223	0.41	51	0.47	51
	3.73		4.11		4.34	
	4.57		4.73		4.77	
$\frac{7}{2}^+$	1.79	209	1.63	47	1.47	47
	5.37		5.34		5.27	

III. WEAK-COUPLING WAVE FUNCTIONS

Weak-coupling calculations in which no T projection is performed can be found in the literature.[4,5] The T-projection techniques used in this work allow an assessment of such an approximation. The results obtained for the two different calculations are shown in Table VII. The weak-coupling dimensions change for ^{20}Ne from an average reduction factor of 2.95 to 1.83. This is to be expected since ^{18}O and ^{18}Ne states will now be distinguishable. Therefore the complete product basis is needed, rather than the lower (or upper) triangular matrix, as used in the previous sections. The difference in energies is typically 5–10 %, which is not negligible for low-lying states.

IV. CONCLUSIONS

A truncation scheme has been applied to ^{20}Ne and ^{21}Ne within an *sd*-shell valence space. A versatile *m*-scheme method has been applied which allows different choices for the starting basis. The building blocks chosen in the present study were the shell-model eigenvectors of neutrons and protons diagonalized separately as distinguishable particles. Product wave functions were formed by directly multiplying the neutron and proton eigenstates and subsequently projecting to obtain good values of J and T for the resulting basis states. Afterwards, the *np* component of the Hamiltonian was applied to this projected basis to couple the neutron and proton subspaces. The overlaps with shell-model wave functions were larger than 0.94 for all the states studied. Although the neutron-proton interaction is strong for these nuclei, it was found that typically only two or three of the overlaps between the eigenstates resulting from the coupling diagonalization and the initial product basis vectors were large.

We note that the present method, based on good-JT bases as building blocks, allows a variety of different initial product bases, not only those generated by solving protons and neutrons separately. It would also be interesting to try other different types of building blocks rather than maximum isospin blocks.

ACKNOWLEDGMENTS

We would like to acknowledge many helpful discussions with Dr. S. T. Hsieh, Dr. P. Halse, Dr. J. B. McGrory, and Dr. B. A. Brown. This work was supported in part by U.S. National Science Foundation Grant PHY 87-18772.

---

*Present address: Departamento de Fisica, Comision Nacional de Energia Atomica, 1429 Buenos Aires, Argentina.

†Present address: Department of Physics and Astronomy, University of New Mexico, Albuquerque, NM 87131.

[1]B. A. Brown and B. H. Wildenthal, Annu. Rev. Nucl. Part. Sci. **38**, 29 (1988).

[2]A. Arima and I. Hamamoto, Annu. Rev. Nucl. Sci. **21**, 55 (1971).

[3]S. S. M. Wong and A. P. Zucker, Phys. Lett. **36B**, 473 (1971).

[4]J. B. McGrory, *Symposium of Shell Model Investigations of Medium-Weight Nuclei* (University of Tokyo, Tokyo, 1977); in *Nuclear Physics*, edited by C. H. Dasso, R. A. Broglia, and A. Winther (North-Holland, Amsterdam, 1982).

[5]H. C. Chiang, M. C. Wang, and S. T. Hsieh, Lett. Nuovo Cimento **34**, 370 (1982); S. T. Hsieh, H. C. Chiang, and M. C. Wang, Nucl. Phys. **A408**, 109 (1983).

[6]A. Etchegoyen, W. D. M. Rae, and N. S. Godwin (MSU version: B. A. Brown, W. E. Ormand, and J. S. Winfield), OXBASH: The Oxford-Buenos Aires Shell-Model Code (unpublished).

[7]R. R. Whitehead *et al.*, Adv. Nucl. Phys. **9**, 123 (1977).

[8]B. H. Wildenthal, Prog. Part. Nucl. Phys. **11**, 5 (1984).